Engineering Journal issn: 0125-8281

Article

Influence of Surface Stresses on the Deflection of Circular Nanoplate with Two-Parameter Elastic Substrate

Supakorn Tirapat[1,a] **and Teerapong Senjuntichai**[2,b,*]

1 Department of Civil Engineering, Faculty of Engineering, Khon Kaen University, Khon Kaen, 40002, Thailand
2 Center of Excellence in Applied Mechanics and Structures, Department of Civil Engineering, Faculty of Engineering, Chulalongkorn University, Bangkok, 10330, Thailand
E-mail: [a]Supati@kku.ac.th, [b,*]Teerapong.S@chula.ac.th (Corresponding author)

Abstract. This paper presents the influence of surface energy effects on the deflection of circular nanoplate with two-parameter elastic substrate. The governing equation for axisymmetric bending of the nanoplate, based on the Gurtin-Murdoch surface elasticity theory, resting on a Winkler-Pasternak elastic foundation is derived from a variational approach based on the concept of minimum total potential energy. The analytical general solution to the governing equation is then obtained in terms of the modified Bessel functions. Finally, closed-form solutions for deflections, bending moment and transverse shear in the nanoplate subjected to normally distributed loading are presented explicitly for the boundary conditions of simple, clamped, and free edges. A set of numerical solutions are selected to demonstrate the influence of surface material parameters and the substrate moduli on the deflection and bending moment profiles of a silicon nanoplate on Winkler-Pasternak foundation. It is found that the nanoplate clearly shows size-dependent behaviors, and becomes stiffer with the existence of surface stresses.

Keywords: Gurtin-Murdoch model, nanoplate, size-dependent, surface energy, Winkler-Pasternak.

ENGINEERING JOURNAL Volume 26 Issue 10
Received 12 July 2022
Accepted 18 October 2022
Published 31 October 2022
Online at https://engj.org/
DOI:10.4186/ej.2022.26.10.99

DOI:10.4186/ej.2022.26.10.99

1. Introduction

Nanoscience has greatly contributed to the development of small-scale structures and devices in various fields including medicine, electronics, fuel cells, solar cell, modern batteries, and chemical sensors. For example, logic and memory devices (LMD) have prompted the creation of novel materials, processes, and technologies to enable the production of more complex devices with sub-micron and nanoscale dimensions. The design of micro-and nano-electromechanical systems (MEMS/NEMS) components requires useful knowledge of physical and mechanical characteristics at the nanoscale level. To improve the performance of such systems, a better understanding of their mechanical behaviors is thus required for the optimum design of nanoscale devices and structures.

The traditional continuum mechanics approach has been widely used to predict and understand the mechanical behavior of nanoscale system throughout the last twenty-five years. Although actual material behavior could be achieved by experiments [1, 2], such findings are still found to be highly reliant on test settings, and the procedure is rather costly due to the need for high-precision equipment. An atomistic investigation revealed that the energy related to atoms near the free surface differ from that in the bulk material [3, 4]. The contribution of surface energy effects then becomes significant for nanoscale structures due to their large surface area to volume ratio, and mechanical behavior becomes size-dependent, which was confirmed according to experimental evidence [1]. Consequently, surface energy effects and size-dependent material behaviors are included in modified continuum-based simulation to represent the behavior of nano-scale systems.

To account for the surface energy effects and size-dependent material behaviors, Gurtin and Murdoch [5, 6] proposed a continuum-based model, known as the surface elasticity theory, which has been applied to various boundary value problems, including elastic fields in layered elastic medium [7], dislocation problems [8], crack problems [9-12], indentation problems [13-15], nanobeams [16, 17], and thin films [18, 19]. In the GM model, a zero-thickness elastic layer perfectly bonded to the bulk material without sliding is characterized as the surface. Several investigations revealed that the GM model can account for nano-scale components accurately [3, 20]. Other continuum-based theories were also proposed, which consider microstructural effects that are usually overlooked in macroscopic continuum theory, and they have been employed to display size-dependent behaviors in various tiny-scale problems, such as the couple stress [21, 22], the strain gradient [23-25], and the nonlocal elasticity [26-33].

Nanoplates are utilized as building blocks in nanocomposites to make micro-and nano-electromechanical (MEM/NEM) devices such as pressure sensors and resonators [34]. Understanding basic characteristics of their behaviors at the nanoscale level is critical for the design optimization of nanometric devices and structures. Mechanical behaviors of these components have thus become a focus of many studies in nanoscience and nanoengineering. Several studies have explored the size-dependent response of nanoplates based on the GM model [3, 18, 19, 34-40]. A theoretical model of a nano-plate supported by an elastic substrate has important applications as it is a simple way to simulate the interaction between two continuous media, such as flexible structural parts in touch with any deformable substrate. Many scientists have studied mechanical behaviors of nanoscale structures sitting on elastic media represented by different forms of substrate models. There are two simplified elastic foundation models that have been widely used in the representation of substrate media. In the first model called the Winkler model [41], the elastic foundation consists of discrete vertical springs that do not account for transverse shear deformation, and the vertical deflection and the contact pressure are proportionally related at a contact point according to the spring stiffness.

Another model, known as the two-parameter model or Winkler-Pasternak model [42], accounts for the impact of shear interaction between the structure and its supporting medium. The application of the two-parameter model has been explored by several researchers in nanomechanics problems. In the context of nanoplates, the size-dependent behavior of a nanoplate on Winkler-Pasternak foundation was investigated by Zenkour and Sobhy [43, 44] based on the nonlocal elasticity theory. Li et al. [45] demonstrated the size-dependent effects of a nanoplate using the modified strain gradient theory. The influence of surface stress effects was also considered by Kamali and Shahabian [46] for the case of a nanoplate supported only on Winkler springs by adopting the GM model. The literature survey reveals that the impact of surface stress on a nano-plate with a Winkler-Pasternak elastic base has never been addressed.

The main objective of the present paper focuses on the bending response of an elastic circular nanoplate sitting on a two-parameter elastic substrate medium under axisymmetric vertical loading and the effect of surface stresses. Other continuum-based theories that take into account microstructural effects are not considered in the present study. The GM elasticity theory [5, 6] and a variational formulation are used to investigate this contact problem. The minimization of the total potential energy yields a differential equation for a circular nanoplate with an elastic base and the contribution of surface energy. By solving the governing equation, closed-form solutions are determined for a uniformly loaded circular nanoplate resting on a Winkler-Pasternak elastic foundation for simple, clamped, and free edges, which can be utilized as a benchmark in the development of numerical approaches for the analysis of nanoplates with arbitrary-shaped or more complex loadings and boundary conditions. Finally, a set of numerical solutions are shown for deflection and bending moment profiles to demonstrate the contribution of surface energy effects on the bending response of nanoplate.

2. Problem Description

Figure 1 shows an elastic circular nanoplate with radius, a, and thickness, h, supported on an elastic substrate under axisymmetric transverse loading $p(r)$. The supporting medium is represented by a two-parameter elastic foundation consisting of the modulus of Winkler foundation, k_w, to portray the vertical stiffness of substrate, and the modulus of Pasternak foundation, G_p, to characterize an incompressible shear layer, which only deforms in transverse shear [41, 42]. Let $w(r)$ be the vertical deflection of a mid-plane of circular nanoplate. The contact pressure, $q(r)$, under the plate on the Pasternak's two-parameter elastic foundation can be represented by,

$$q(r) = k_w w(r) - G_p\left(\frac{\partial^2 w(r)}{\partial r^2} + \frac{1}{r}\frac{\partial w(r)}{\partial r}\right) \tag{1}$$

Under an axisymmetric deformation, the displacement components of a Kirchhoff plate of uniform thickness can be expressed as follows:

$$u_r = -z\frac{dw(r)}{dr};\quad u_z = w(r) \tag{2}$$

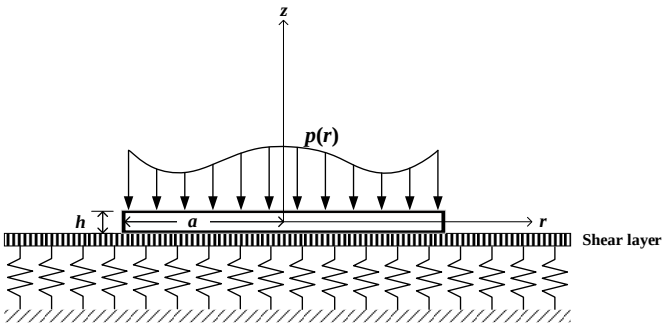

Fig. 1. Circular nanoplate on two- parameter elastic substrate medium.

To integrate the surface energy influence into the bending of nanoplate, the Gurtin and Murdoch's continuum theory [5, 6] is then adopted. According to the GM model, the plate consists of an elastic surface with mathematically zero thickness that is completely bonded to the bulk material. The governing equations for the bulk are taken from the traditional theory of elastic plates [47]. For the surface, the constitutive relations and strain-displacement relationship can respectively be stated as [5, 6],

$$\sigma_{rr}^s = \tau^s + \left(2\mu^s + \lambda^s\right)\varepsilon_{rr}^s + \left(\lambda^s + \tau^s\right)\varepsilon_{\theta\theta}^s \tag{3}$$

$$\sigma_{\theta\theta}^s = \tau^s + \left(2\mu^s + \lambda^s\right)\varepsilon_{\theta\theta}^s + \left(\lambda^s + \tau^s\right)\varepsilon_{rr}^s \tag{4}$$

$$\sigma_{zr}^s = \tau^s\frac{du_z^s}{dr} \tag{5}$$

$$\varepsilon_{rr}^s = \frac{du_r^s}{dr};\qquad \varepsilon_{\theta\theta}^s = \frac{u_r^s}{r} \tag{6}$$

where the superscript "s" denotes parameters related to the surface; λ^s and μ^s denote surface Lamé constants; and τ^s is the residual surface stress (or residual surface tension) under unstrained conditions, and it is assumed to be constant.

The normal (out-of-plane) stress σ_{zz} is disregarded in the classical theory of thin plates since it is negligible when compared to other stress components. Under the surface stress effects, the bulk stress tensor σ_{zz} is assumed to linearly vary along the plate thickness, h, to fulfill the equilibrium requirements along the interface, and σ_{zz} can then be written as [19, 34],

$$\sigma_{zz} = \frac{1}{2}\left(\sigma_{zz}^+ + \sigma_{zz}^-\right) + \frac{z}{h}\left(\sigma_{zz}^+ - \sigma_{zz}^-\right) \tag{7}$$

where σ_{zz}^+ and σ_{zz}^- respectively represent the out-of-plane stresses that exert on the top and bottom surfaces of the plate. In addition, Young-Laplace equation for the top and bottom surfaces can be expressed as [36]

$$\frac{\partial\sigma_{zr}^{s\pm}}{\partial r} + \frac{\sigma_{zr}^{s\pm}}{r} \mp \sigma_{zz}^{\pm} = 0 \tag{8}$$

where σ_{zr}^{s+} and σ_{zr}^{s-} respectively denote the stresses at the top and bottom surfaces of the nanoplate. Based on Eqs. (7) and (8), the bulk stress σ_{zz} in the nanoplate based on the GM model can then be written as,

$$\sigma_{zz} = \frac{2\tau^s z}{h}\left(\frac{d^2w(r)}{dr^2} + \frac{1}{r}\frac{dw(r)}{dr}\right) \tag{9}$$

In view of Eqs. (2) to (6), the normal stresses σ_{rr} and $\sigma_{\theta\theta}$ can also be expressed in terms of $w(r)$ as,

$$\begin{aligned}\sigma_{rr} = {} & \frac{E}{1+\nu}\left[\frac{1}{1-\nu}\left(-z\frac{d^2w(r)}{dr^2}\right) + \frac{\nu}{1-\nu}\left(-\frac{z}{r}\frac{dw(r)}{dr}\right)\right] \\ & + \frac{\nu}{1-\nu}\frac{2\tau^s z}{h}\left(\frac{d^2w(r)}{dr^2} + \frac{1}{r}\frac{dw(r)}{dr}\right)\end{aligned} \tag{10}$$

$$\begin{aligned}\sigma_{\theta\theta} = {} & \frac{E}{1+\nu}\left[\frac{1}{1-\nu}\left(-\frac{z}{r}\frac{dw(r)}{dr}\right) + \frac{\nu}{1-\nu}\left(-z\frac{d^2w(r)}{dr^2}\right)\right] \\ & + \frac{\nu}{1-\nu}\frac{2\tau^s z}{h}\left(\frac{d^2w(r)}{dr^2} + \frac{1}{r}\frac{dw(r)}{dr}\right)\end{aligned} \tag{11}$$

where E and ν are Young's modulus and Poisson's ratio of the bulk material of nanoplate respectively.

3. Governing Equations and General Solutions

The governing equilibrium equation of a circular nanoplate overlying a two-parameter elastic substrate medium as illustrated in Fig. 1 can be established using a variational technique [47, 48]. Let a total potential energy of the nanoplate-substrate system in Fig. 1, denoted by Π, be written as,

$$\Pi = U_B + U_s + U_F + W \tag{12}$$

where U_B, U_S, and U_F represent the elastic strain energies in the bulk material of nanoplate, in the surface of nanoplate, and in the Winkler-Pasternak foundation respectively. In addition, W represents the potential energy due to a distributed load, $p(r)$. The above variables in Eq. (12) are given by,

$$U_B = \frac{1}{2}\int_V \left(\sigma_{rr}\varepsilon_{rr} + \sigma_{\theta\theta}\varepsilon_{\theta\theta}\right)dV \tag{13}$$

$$U_s = \frac{1}{2}\int_\Gamma \left(\sigma_{rr}^{s\pm}\varepsilon_{rr}^{s\pm} + \sigma_{\theta\theta}^{s\pm}\varepsilon_{\theta\theta}^{s\pm} + 2\sigma_{zr}^{s\pm}\varepsilon_{zr}^{s\pm}\right)d\Gamma \tag{14}$$

$$U_F = \frac{1}{2}\int_0^{2\pi}\int_0^a q(r)\cdot w(r)\cdot r dr d\theta \tag{15}$$

$$W = -\frac{1}{2}\int_0^{2\pi}\int_0^a p(r)\cdot w(r)\cdot r dr d\theta \tag{16}$$

where V and Γ respectively denote the bulk volume and surface area of nanoplate, and $q(r)$ denotes the contact pressure from the Pasternak elastic foundation given by Eq. (1).

It can be shown that the total potential energy of the system shown in Fig. 1 is expressed as,

$$\begin{aligned}\Pi = \pi\int_0^a &\left\{\frac{Eh^3}{12(1-\nu^2)}\left[\left(\frac{\partial^2 w}{\partial r^2}+\frac{1}{r}\frac{\partial w}{\partial r}\right)^2 - \frac{2(1-\nu)}{r}\frac{\partial^2 w}{\partial r^2}\frac{\partial w}{\partial r}\right]\right.\\ &\left.-\frac{\tau^s \nu h^2}{6(1-\nu)}\left(\frac{\partial^2 w}{\partial r^2}+\frac{1}{r}\frac{\partial w}{\partial r}\right)^2\right\} r dr\\ +\pi\int_0^a &\left\{\left(\lambda^s+2\mu^s\right)\frac{h^2}{2}\left(\left(\frac{\partial^2 w}{\partial r^2}\right)^2+\left(\frac{1}{r}\frac{\partial w}{\partial r}\right)^2\right)\right.\\ &\left.+2\tau^s\left(\frac{\partial w}{\partial r}\right)^2+\left(\lambda^s+\tau^s\right)h^2\left(\frac{1}{r}\frac{\partial w}{\partial r}\right)\left(\frac{\partial^2 w}{\partial r^2}\right)\right\} r dr\\ +\pi\int_0^a &\left\{k_w w^2 - G_p w\left(\frac{\partial^2 w}{\partial r^2}+\frac{1}{r}\frac{\partial w}{\partial r}\right)\right\} r dr - \pi\int_0^a p(r)\cdot w(r) r dr\end{aligned} \tag{17}$$

The minimization of the total potential energy given by Eq. (17) together with the subsequent integration by parts yields the following governing equation for a circular nanoplate sitting on a two-parameter elastic substrate medium.

$$\bar{D}\nabla^4 w - \bar{G}\nabla^2 w + k_w w = p(r) \tag{18}$$

where $\nabla^2 = \frac{1}{r}\frac{\partial}{\partial r}\left(r\frac{\partial}{\partial r}\right)$ is the Laplace operator, and

$$\bar{D} = D + \left(\lambda^s + 2\mu^s\right)\frac{h^2}{2} - \frac{\tau^s \nu h^2}{6(1-\nu)} \tag{19}$$

$$\bar{G} = G_p + 2\tau^s \tag{20}$$

In addition, $D = \frac{Eh^3}{12(1-\nu^2)}$ represents the flexural rigidity of an elastic plate [47].

The bending moment and shearing force respectively of a circular nanoplate are shown below.

$$M_r = \bar{D}\frac{\partial^2 w}{\partial r^2} + \frac{\bar{D}_1}{r}\frac{\partial w}{\partial r} \tag{21}$$

$$Q_r = -\bar{D}\frac{\partial}{\partial r}\nabla^2 w + 2\tau^s\frac{\partial w}{\partial r} \tag{22}$$

where

$$\bar{D}_1 = \nu D - \frac{\tau^s \nu h^2}{6(1-\nu)} + \left(\lambda^s + \tau^s\right)\frac{h^2}{2} \tag{23}$$

When the surface energy influence is ignored, the Eq. (18) is simplified to the governing equation of a circular plate on a two-parameter foundation [49]. On the other hand, if the two-parameter elastic model (k_w and G_p) is discarded from the present model, Eqs. (18) to (23) are reduced to the bending equation of a circular nanoplate, which was derived from the equilibrium of an infinitesimal plate element [36]. The classical Kirchhoff equation for the plate bending can also be obtained from the current study by neglecting both elastic substrate and the influence of surface stresses (i.e., the parameters k_w and G_p as well as τ^s, λ^s, and μ^s are all set to be zero).

The complete solution of the governing equation, Eq. (18), is a sum of a complementary function, w_c, and a particular integral, w_p. Two different forms of w_c exist depending on the condition of $\left(\bar{G}/\bar{D}\right)^2 - 4k_w/\bar{D}$. If $\left(\bar{G}/\bar{D}\right)^2 - 4k_w/\bar{D}$ is non-negative, i.e., the interaction between the plate and the substrate is controlled by the shear layer, the complementary function can be written as [48-50]

$$w_c(r) = C_1 I_0(\alpha_1 r) + C_2 I_0(\alpha_2 r) + C_3 K_0(\alpha_1 r) + C_4 K_0(\alpha_2 r) \tag{24}$$

and

$$\begin{Bmatrix}\alpha_1^2\\ \alpha_2^2\end{Bmatrix} = \frac{1}{2}\left\{\frac{\bar{G}}{\bar{D}} \pm \sqrt{\left(\frac{\bar{G}}{\bar{D}}\right)^2 - 4\frac{k_w}{\bar{D}}}\right\} \tag{25}$$

where I_0 and K_0 denote the modified Bessel function of the first and second kind respectively [50], and C_1 to C_4 are the arbitrary constants that can be determined from the boundary conditions.

When $\left(\bar{G}/\bar{D}\right)^2 - 4k_w/\bar{D}$ is negative for the case where the vertical stiffness characterized by vertical springs in the substrate model is a predominant parameter, α_1^2 and α_2^2 become complex conjugates, and the solution of w_c then becomes,

$$w_c(r) = C_1 I_0(\alpha r)_r + C_2 I_0(\alpha r)_i + C_3 K_0(\alpha r)_r + C_4 K_0(\alpha r)_i \tag{26}$$

where the subscripts r and i are used to denote the real and imaginary parts of the Bessel functions respectively.

Note that for the case of Winkler spring foundation $(G \equiv 0)$, the four Bessel functions in Eq. (26) are reduced to the ber, bei, ker, and kei functions [50], and the solution of w_c is given by,

$$w_c(r) = C_1 ber(\alpha r) + C_2 bei(\alpha r) + C_3 ker(\alpha r) + C_4 kei(\alpha r) \tag{27}$$

4. Closed-form Solution for Uniformly Loaded Nanoplate

Consider a circular nanoplate sitting on a two-parameter elastic substrate as shown in Fig. 1. Generally, the substrate medium is dominated by the vertical stiffness (k_w) thus $\left(\bar{G}/\bar{D}\right)^2 < 4k_w/\bar{D}$ in Eq. (25). The solution of w_c is then given by Eq. (26). To satisfy the condition of zero slope and zero shearing force at the center of the plate, C_3 and C_4 are set to zero in Eq. (26) to avoid a logarithmic singularity as $r \to 0$ due to the presence of the Bessel function K_0. Let the plate be subjected to a uniformly distributed load of intensity p_0 over its entire area. The particular integral for this case is given by $w_p = -p_0/k_w$, and the complete solution of the nanoplate-substrate system shown in Fig. 1 then becomes

$$w(r) = C_1 I_0(\alpha r)_r + C_2 I_0(\alpha r)_i - \frac{p_0}{k_w} \tag{28}$$

To determine the two arbitrary constants, C_1 and C_2, the following equations are applied to represent different boundary conditions at the plate edge.

(i) Simply-supported boundary:

$$w(r)\big|_{r=a} \quad \text{and} \quad M_r\big|_{r=a} = 0 \tag{29}$$

(ii) Built-in or clamped boundary:

$$w(r)\big|_{r=a} \quad \text{and} \quad \frac{\partial w}{\partial r}\bigg|_{r=a} = 0 \tag{30}$$

(iii) Free-edge boundary:

$$M_r\big|_{r=a} = 0 \quad \text{and} \quad Q_r\big|_{r=a} = G_p\left(\frac{\partial w_f}{\partial r} - \frac{\partial w}{\partial r}\right)_{r=a} \tag{31}$$

$$w(r)\big|_{r=a} = w_f(r)\big|_{r=a} \tag{32}$$

where $w_f(r)$ denotes the deflected shape of the substrate medium, which is obtained by solving the following homogeneous differential equation beyond the plate edge [48].

$$G_p \nabla^2 w_f(r) - k_w w_f(r) = 0 \quad \text{for} \quad a < r < \infty \tag{33}$$

The second condition in Eq. (31) for free-edge boundary accounts for the effect of the shearing stresses in both the substrate medium and the nanoplate. Besides, Eq. (32) is also imposed to ensure the continuity of displacements (between plate and substrate) at the plate edge. The solution for Eq. (33) is given by

$$w_f(r) = C_5 I_0(\chi r) + C_6 K_0(\chi r) \tag{34}$$

where C_5 and C_6 are arbitrary constants, and $\chi = \sqrt{k_w/G_p}$. Note that the constant C_5 is ignored in Eq. (34) to avoid the singularity in the solution due to the Bessel function I_0.

Substituting Eq. (28) into Eqs. (21) and (22) yields the solutions for slope, bending moment, and shearing force of the nanoplate respectively as follows:

$$\frac{\partial w}{\partial r} = C_1\left(\beta I_1(\alpha r)_r - \gamma I_1(\alpha r)_i\right) + C_2\left(\beta I_1(\alpha r)_i + \gamma I_1(\alpha r)_r\right) \tag{35}$$

$$\begin{aligned} M_r = {} & \bar{D}\begin{Bmatrix} C_1\left(\left(\beta^2-\gamma^2\right) I_0(\alpha r)_r - 2\beta\gamma I_0(\alpha r)_i\right) \\ +C_2\left(\left(\beta^2-\gamma^2\right) I_0(\alpha r)_i + 2\beta\gamma I_0(\alpha r)_r\right) \end{Bmatrix} \\ & +\bar{D}\begin{Bmatrix} C_1\left(-\frac{\beta}{r} I_1(\alpha r)_r + \frac{\gamma}{r} I_1(\alpha r)_i\right) \\ +C_2\left(-\frac{\beta}{r} I_1(\alpha r)_i - \frac{\gamma}{r} I_1(\alpha r)_r\right) \end{Bmatrix} \\ & +\bar{D}_1\begin{Bmatrix} C_1\left(\frac{\beta}{r} I_1(\alpha r)_r - \frac{\gamma}{r} I_1(\alpha r)_i\right) \\ +C_2\left(\frac{\beta}{r} I_1(\alpha r)_i + \frac{\gamma}{r} I_1(\alpha r)_r\right) \end{Bmatrix} \end{aligned} \tag{36}$$

$$\begin{aligned} Q_r = {} & -\bar{D}C_1\begin{pmatrix} \left(\beta^2-\gamma^2\right)\left[\beta I_1(\alpha r)_r - \gamma I_1(\alpha r)_i\right] \\ -2\beta\gamma\left[\beta I_1(\alpha r)_i + \gamma I_1(\alpha r)_r\right] \end{pmatrix} \\ & -\bar{D}C_2\begin{pmatrix} \left(\beta^2-\gamma^2\right)\left[\beta I_1(\alpha r)_i + \gamma I_1(\alpha r)_r\right] \\ +2\beta\gamma\left[\beta I_1(\alpha r)_r - \gamma I_1(\alpha r)_i\right] \end{pmatrix} \\ & +2\tau^s\begin{pmatrix} C_1\left(\beta I_1(\alpha r)_r - \gamma I_1(\alpha r)_i\right) \\ +C_2\left(\beta I_1(\alpha r)_i + \gamma I_1(\alpha r)_r\right) \end{pmatrix} \end{aligned} \tag{37}$$

where β and γ denote the real and imaginary parts of the parameter α respectively.

In view of Eqs. (28), (29) and (36), the arbitrary constants C_1 and C_2 corresponding to the case of a simply-supported nanoplate under uniform loading are given by,

$$C_1 = \frac{p_0}{k_w} \cdot \frac{A_4}{A_1 A_4 - A_2 A_3} \tag{38}$$

$$C_2 = \frac{p_0}{k_w} \cdot \frac{-A_3}{A_1 A_4 - A_2 A_3} \tag{39}$$

where

$$A_1 = I_0(\alpha a)_r; \qquad A_2 = I_0(\alpha a)_i \tag{40}$$

$$A_3 = \bar{D}\left(\left(\beta^2-\gamma^2\right) I_0(\alpha a)_r - 2\beta\gamma I_0(\alpha a)_i - \frac{\beta}{a} I_1(\alpha a)_r + \frac{\gamma}{a} I_1(\alpha a)_i\right) + \bar{D}_1\left(\frac{\beta}{a} I_1(\alpha a)_r - \frac{\gamma}{a} I_1(\alpha a)_i\right) \tag{41}$$

$$A_4 = \bar{D}\left(\left(\beta^2-\gamma^2\right) I_0(\alpha a)_i + 2\beta\gamma I_0(\alpha a)_r - \frac{\beta}{a} I_1(\alpha a)_i - \frac{\gamma}{a} I_1(\alpha a)_r\right) + \bar{D}_1\left(\frac{\beta}{a} I_1(\alpha a)_i + \frac{\gamma}{a} I_1(\alpha a)_r\right) \tag{42}$$

Similarly, the arbitrary constants C_1 and C_2 corresponding to the case of a built-in nanoplate can be determined from Eqs. (28), (30) and (35), and they are given as follows:

$$C_1 = \frac{\left(p_0/k_w\right)\cdot\left(\beta I_1(\alpha a)_i + \gamma I_1(\alpha a)_r\right)}{A_1\cdot\left(\beta I_1(\alpha a)_i + \gamma I_1(\alpha a)_r\right) - A_2\cdot\left(\beta I_1(\alpha a)_r - \gamma I_1(\alpha a)_i\right)} \tag{43}$$

$$C_2 = \frac{\left(p_0/k_w\right)\cdot\left(-\beta I_1(\alpha a)_r + \gamma I_1(\alpha a)_i\right)}{A_1\cdot\left(\beta I_1(\alpha a)_i + \gamma I_1(\alpha a)_r\right) - A_2\cdot\left(\beta I_1(\alpha a)_r - \gamma I_1(\alpha a)_i\right)} \tag{44}$$

Finally, the arbitrary functions are obtained from Eqs. (28), (31), (32), and (34) – (37) for the case where the edge of the nanoplate is free from any restraint, and they are given by,

$$C_1 = \frac{\left(p_0/k_w\right)\cdot\left(A_4 G_p \chi K_1(\chi a)\right)}{-G_p \chi K_1(\chi a)\left[A_3A_2 - A_4A_1\right] - K_0(\chi a)\left[A_3A_6 - A_4A_5\right]} \tag{45}$$

$$C_2 = \frac{\left(p_0/k_w\right)\cdot\left(-A_3 G_p \chi K_1(\chi a)\right)}{-G_p \chi K_1(\chi a)\left[A_3A_2 - A_4A_1\right] - K_0(\chi a)\left[A_3A_6 - A_4A_5\right]} \tag{46}$$

$$C_6 = \frac{\left(p_0/k_w\right)\cdot\left(A_3A_6 - A_4A_5\right)}{-G_p \chi K_1(\chi a)\left[A_3A_2 - A_4A_1\right] - K_0(\chi a)\left[A_3A_6 - A_4A_5\right]} \tag{47}$$

where

$$A_5 = \bar{D}\left(-\left[\beta\left(\beta^2-\gamma^2\right)-2\beta\gamma^2\right]I_1(\alpha a)_r + \left[\gamma\left(\beta^2-\gamma^2\right)+2\beta^2\gamma\right]I_1(\alpha a)_i\right) + \left(2\tau^s + G_p\right)\left(\beta I_1(\alpha a)_r - \gamma I_1(\alpha a)_i\right) \tag{48}$$

$$A_6 = \bar{D}\left(-\left[\beta\left(\beta^2-\gamma^2\right)-2\beta\gamma^2\right]I_1(\alpha a)_i - \left[\gamma\left(\beta^2-\gamma^2\right)+2\beta^2\gamma\right]I_1(\alpha a)_r\right) + \left(2\tau^s + G_p\right)\left(\beta I_1(\alpha a)_i + \gamma I_1(\alpha a)_r\right) \tag{49}$$

5. Numerical Results

Explicit expressions for vertical deflection, bending moment and shear of the nanoplate sitting on a two-parameter elastic substrate medium under uniformly distributed loading are given in the preceding section. The following normalized parameters are employed in the display of numerical solutions:

$$K^* = \frac{k_w a^4}{D} \quad \text{and} \quad G^* = \frac{G_p a^2}{D} \tag{50}$$

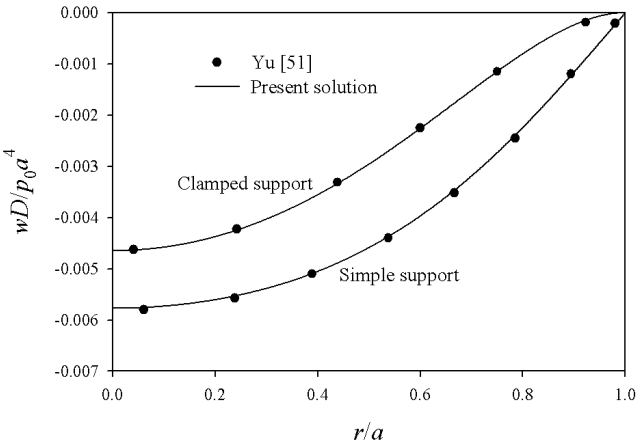

Fig. 2. Comparisons for normalized deflection of a circular plate on two-parameter elastic substrate medium without surface energy effects.

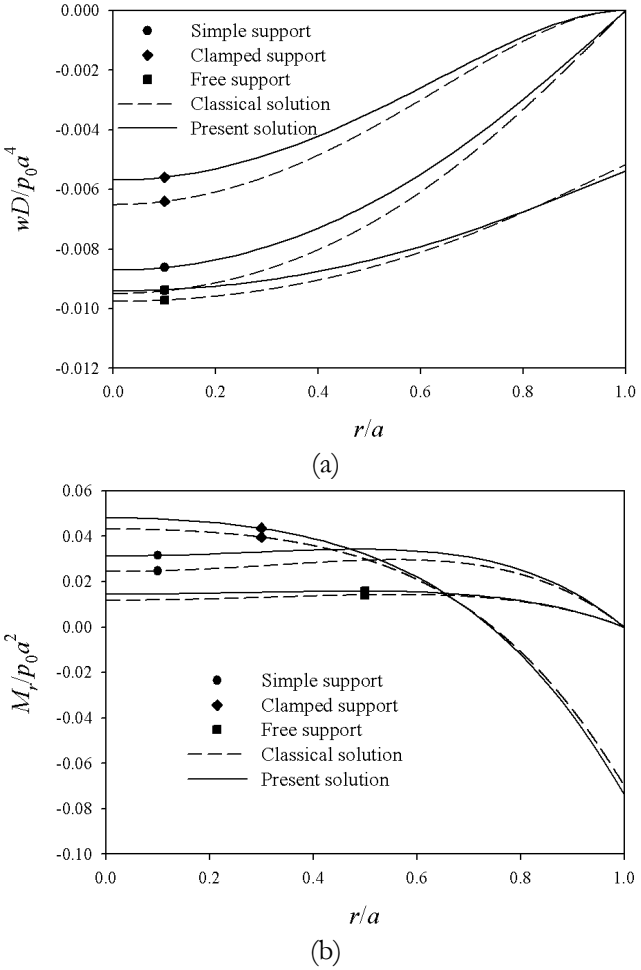

Fig. 3. Profiles of (a) normalized deflection and (b) normalized bending moment of a uniformly loaded circular nanoplate on two-parameter elastic substrate.

To verify the validity of the derived analytical solution, the comparison with existing solutions for a limited case of a circular plate on a two-parameter elastic substrate medium is performed. Figure 2 illustrates a comparison of normalized deflection profiles of a circular plate under constant loading p_0 between the current solution, without the contribution of surface energy effects (by setting λ^s, μ^s and $\tau^s \cong 0$), and the analytical solution proposed by Yu [51]. The circular plate, with a radius of 10 m and a rigidity modulus of $D = 10^6$ N·m, is considered for two types of boundary conditions, simple and clamped edges, and a uniform pressure of $p_0 = 1$ kPa. In addition, the normalized values of the moduli of Winkler and Pasternak foundations are defined respectively as $K^* = 200$ and $G^* = 3$. It is obvious from Fig. 2 that the plate deflection profiles from the two solutions agree very well along the plate radius for both simple and clamped supports.

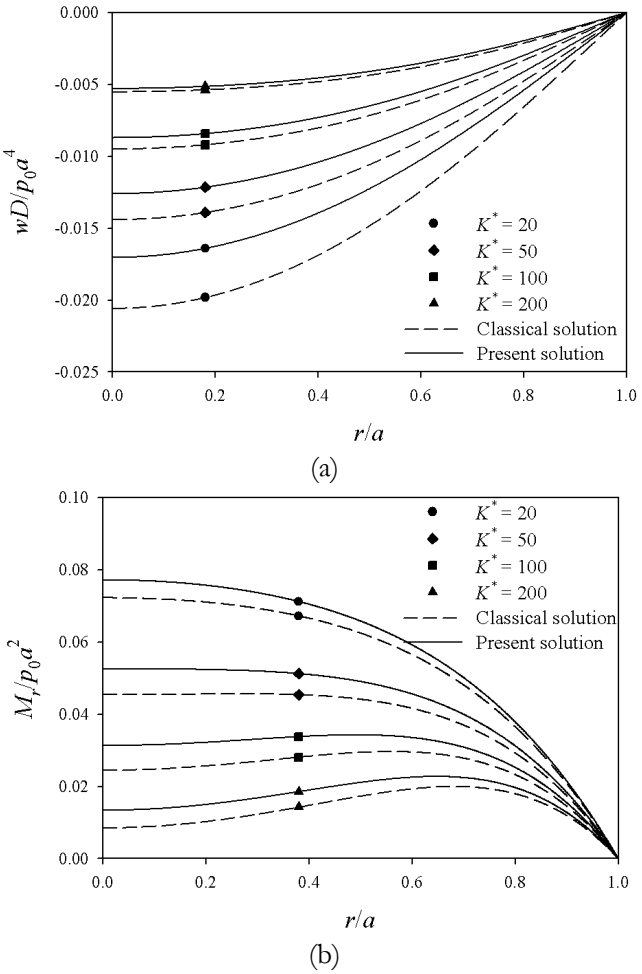

Fig. 4. Profiles of (a) normalized vertical deflection and (b) normalized bending moment of a uniformly loaded circular nanoplate with simple support on two-parameter elastic substrate for different values of K^*.

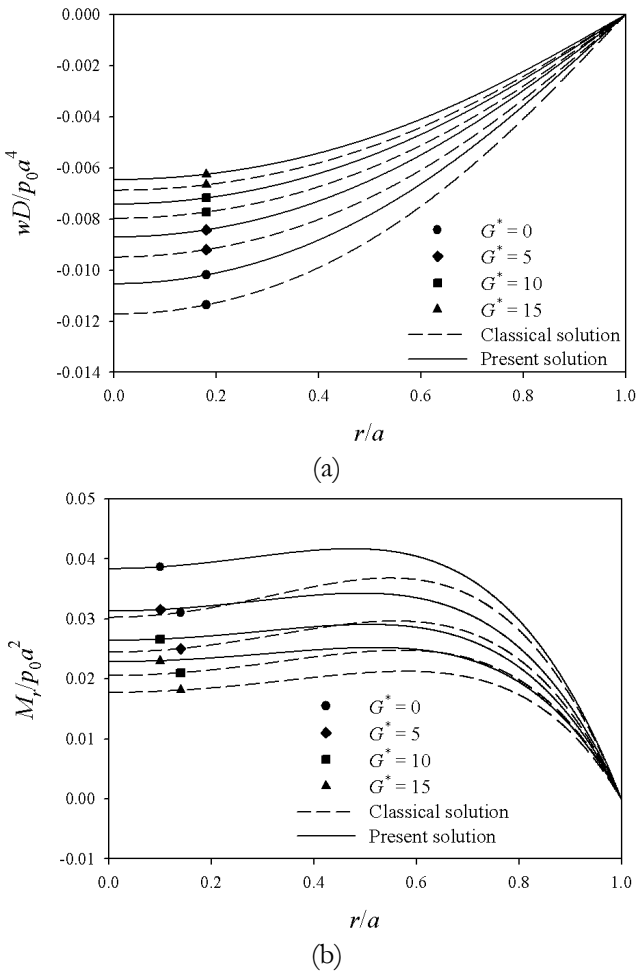

Fig. 5. Profiles of (a) normalized vertical deflection and (b) normalized bending moment of a uniformly loaded circular nanoplate with simple support on two-parameter elastic substrate for different values of G^*.

The contribution of surface stress effects on flexural behaviors of a circular nanoplate lying on a two-parameter elastic substrate medium is explored next by considering the case of a silicon nanoplate. The bulk and surface material parameters of silicon were obtained from atomistic simulations [52]. The surface material values are defined as $\lambda^s = 4.4939$ N/m, $\mu^s = 2.7779$ N/m, and $\tau^s = 0.6056$ N/m while the bulk properties are $E = 107$ GPa and $\nu = 0.33$ for the nanoplate. To illustrate the surface energy influence, the corresponding classical solutions (λ^s, μ^s and $\tau^s \cong 0$) are also presented in all figures in this section with the broken lines.

Figures 3 (a) and 3 (b) respectively show the radial profiles of normalized deflections and bending moments of a circular silicon plate, with $a = 10$ nm and $h = 2$ nm, sitting on a two-parameter elastic substrate medium ($K^* = 100$ and $G^* = 5$) under a constant external load, p_0 and simple, clamped, and free supports. Due to the boundary conditions, the deflections at the simple and clamped supports are zero, and the bending moments are then vanished along the simple and free supports as shown in Figs. 3(a) and 3(b) respectively. It is also found that the maximum central deflection occurs in the nanoplate with the free support, followed by the simple and clamped supports respectively. In addition, the maximum mid-span bending moment is observed in the clamped plate whereas the free-supported plate yields the minimum moment. It is also evident from both Figs. 3 (a) and 3 (b) that although the current and classical elasticity solutions show comparable patterns for both normalized deflections and bending moments and all boundary conditions, a significant influence from the surface energy is illustrated in the difference between both solutions, especially near the nanoplate center. Besides, Figure 3 (a) shows that the normalized deflection of the nanoplate is lower than the classical plate deflection but the normalized bending

DOI:10.4186/ej.2022.26.10.99

moment under the impact of surface stresses is higher in the Fig. 3 (b) implying that the existence of surface stresses renders the nanoplate stiffer under all support situations.

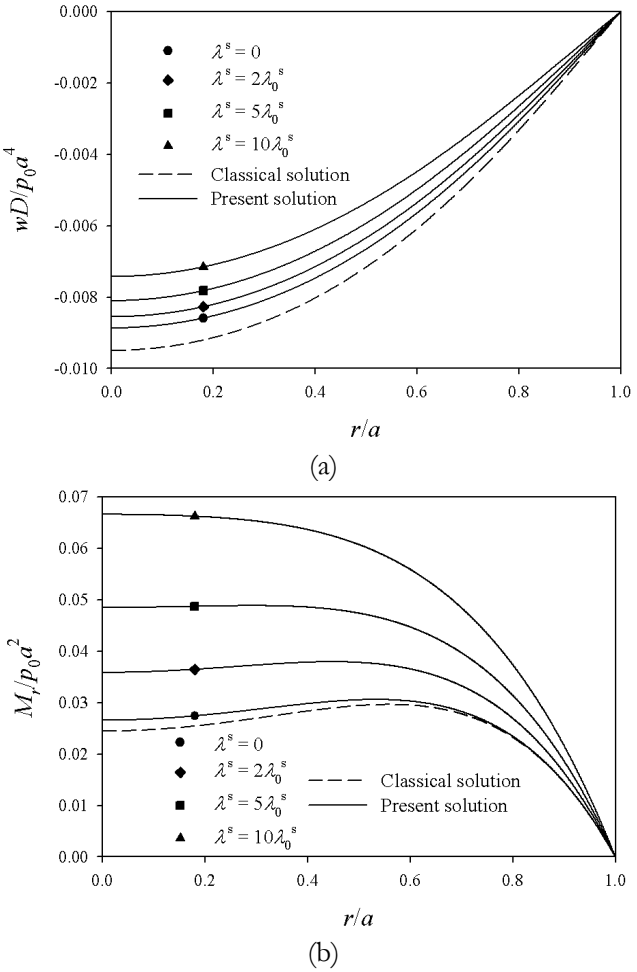

Fig. 6. Profiles of (a) normalized vertical deflection and (b) normalized bending moment of a uniformly loaded circular nanoplate with simple support on two-parameter elastic substrate for different values of λ^s.

Next, the effects of substrate parameters on the bending of circular nanoplate are examined via the deflection and bending moment profiles of the nanoplate. Figures 4 and 5 show the influence of substrate moduli K^* and G^* respectively on a uniformly loaded silicon plate, with a = 10 nm, h = 2 nm and simply-supported edge, lying on a two-parameter elastic substrate. In Figs. 4 and 5, four different values of K^* are considered, i.e., K^* = 20, 50, 100 and 200, whereas the values of G^* are varied from 0 to 15. The values of K^* are selected to fall within the typical range of K^* employed in previous studies on nanoplates on elastic substrate [36, 43-46]. In addition, the values of G^* are chosen to represent a common substrate medium that is dominated by the vertical stiffness, and the complete solution of the nanoplate deflection is then given by Eq. (28). A significant contribution from the surface energy effects on the normalized deflection and bending moment of nanoplate is once again evident from Figs. 4 and 5. A nanoplate becomes stiffer, i.e., the plate deflection is reduced but the bending moment increases, with the existence of surface stresses. Furthermore, the radial profiles shown in Figs. 4 and 5 reveal that normalized plate deflections and bending moment decreases with the increment of the substrate parameters K^* and G^* respectively. The bending response of nanoplate thus shows a significant dependence on the two substrate parameters.

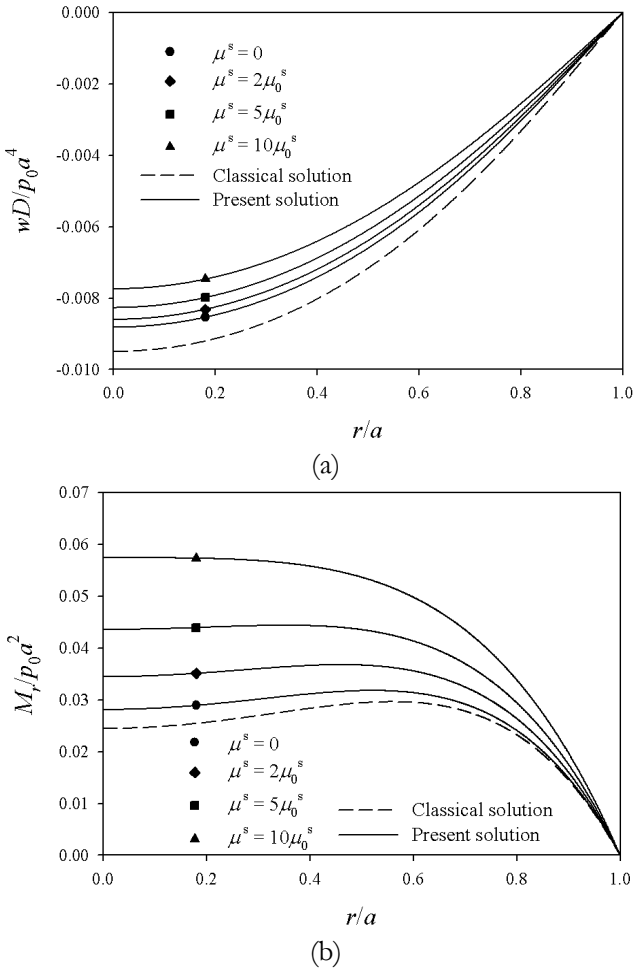

Fig. 7. Profiles of (a) normalized vertical deflection and (b) normalized bending moment of a uniformly loaded circular nanoplate with simple support on two-parameter elastic substrate for different values of μ^s.

In Figs. 6 to 8, the influence of surface parameters on flexural behaviors of a circular nanoplate with simply-supported edge lying on a two-parameter elastic substrate medium is investigated. The normalized values of the moduli of Winkler foundation and Pasternak foundation remain unchanged (K^* = 100 and G^* = 5) and τ^s = 0.6056 N/m for the silicon plate with a = 10 nm and h = 2 nm. Figures 6 and 7 show radial profiles of normalized deflection and bending moment for different values of surface Lamé constants with λ_0^s = 4.4939 N/m and μ_0^s = 2.7779 N/m. The numerical results for the current study and the classical solution in Figs. 6 and 7 exhibit similar trends for both the deflections and bending moments at various values of surface Lamé constants, λ^s and μ^s. Apparently, the present solution clearly produces smaller deflections but higher bending moments (i.e., the

nanoplate is strengthened) by raising the values of either λ^s or μ^s.

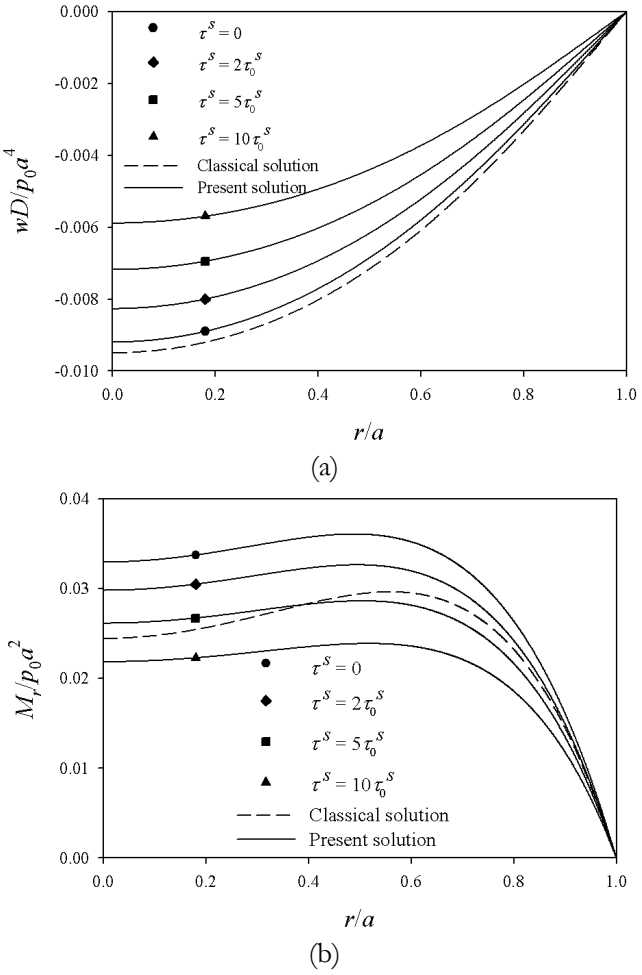

Fig. 8. Profiles of (a) normalized vertical deflection and (b) normalized bending moment of a uniformly loaded circular nanoplate with simple support on two-parameter elastic substrate for different values of τ^s.

Figure 8 shows the effects of residual surface stress, τ^s, on the deflection and bending moment of the nanoplate. The values of τ^s are varied, i.e., $\tau_0^s = 0$, $2\tau_0^s$, $5\tau_0^s$, $10\tau_0^s$ when τ_0^s = 0.6056 N/m, with other material parameters unchanged. Similar to what observed from the influence of surface Lamé constants in Figs. 6 (a) and 7 (a), the deflection of the nanoplate in Fig. 8 (a) is smaller than the classical solution due to the surface stress effects, and the deflection is reduced with increasing the values of residual surface tension τ^s. However, unlike the cases of surface Lamé constants, λ^s and μ^s illustrated in Figs. 6 (b) and 7 (b) respectively, the bending moment of nanoplate decreases with increasing the values of τ^s as shown in Fig. 8 (b). This is due to the fact that the residual surface tension has an adverse effect on the flexural rigidity of nanoplate (see Eqs. (19) and (23)) thus, by increasing the value of τ^s, the nanoplate becomes more flexible, and the bending moment is then reduced. Besides, it is also found that the bending moment from the current study becomes smaller than the corresponding classical solution when $\tau^s > 5\tau_0^s$.

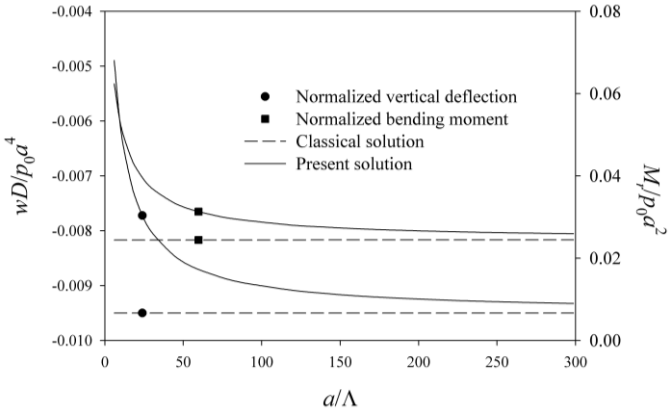

Fig. 9. Variations of normalized central deflection and normalized bending moment with the normalized plate radius a/Λ for a uniformly loaded circular nanoplate with simple support on two-parameter elastic substrate.

The final set of the numerical solutions highlights the size-dependent behavior of the nanoplate when the existence of surface energy effects is detected with the surface material characteristics given by λ^s = 4.4939 N/m, μ^s = 2.7779 N/m, and τ^s = 0.6056 N/m. In addition, $\Lambda = \kappa^s(\lambda + 2\mu)/2\mu(\lambda + \mu)$ is a characteristic length of the nanoplate where $\kappa^s = \lambda^s + 2\mu^s$, l and m denote Lamè constants of the bulk material of nanoplate, and L = 0.1674 nm for silicon nanoplate. Figure 9 depicts the radial variation of deflection and bending moment of a uniformly loaded nanoplate with a simply-supported edge. Under the impact of surface stresses, a size-dependent behavior in the bending response of nanoplate is obvious from Fig. 9 with the normalized deflection and bending moment highly dependent on the normalized plate radius a/Λ. As the normalized radius of the nanoplate increases, the current solution that accounts for surface energy effects converges to the classical counterpart, which is clearly size-independent.

6. Conclusions

This work examines the influence of surface energy effects on an elastic circular nanoplate sitting on a two-parameter elastic substrate medium under axisymmetric transverse loading by adopting the GM surface elasticity theory and a variational formulation. Closed-form analytical solution for this contact problem is successfully derived for a uniformly loaded nanoplate with simple, clamped, and free supports. Numerical solutions presented in this paper indicate that the bending of the nanoplate depends significantly on the influence of surface energy effects and the substrate moduli. Under the surface stresses, the nanoplate deflection decreases by increasing each surface material constant. The normalized bending moment increases with increasing the surface Lamé constants, but it is reduced when the residual surface

tension increases. In addition, the nanoplate exhibits a size-dependent behavior in bending due to the existence of surface energy effects. The size-dependent behavior vanishes as the radius of nanoplate increases, and the current results finally converge to the classical counterparts.

Acknowledgement

This work (Grant no. RGNS 63-056) was financially supported by Office of the Permanent Secretary, Ministry of Higher Education, Science, Research and Innovation. The support is gratefully acknowledged.

References

[1] E. W. Wong, P. E. Sheehan, and C. M. Lieber, "Nanobeam mechanics: Elasticity, strength, and toughness of nanorods and nanotubes," *Science*, vol. 277, no. 5334, pp. 1971–1975, 1997.

[2] S. X. Mao, M. Zhao, and Z. L. Wang, "Nanoscale mechanical behavior of individual semiconducting nanobelts," *Applied Physics Letters*, vol. 83, no. 5, pp. 993–995, 2003.

[3] R. E. Miller and V. B. Shenoy, "Size-dependent elastic properties of nanosized structural elements," *Nanotechnology*, vol. 11, no. 3, p. 139, 2000.

[4] V. B. Shenoy, "Size-dependent rigidities of nanosized torsional elements," *International Journal of Solids and Structures*, vol. 39, no. 15, pp. 4039–4052, 2002.

[5] M. E. Gurtin and A. Ian Murdoch, "A continuum theory of elastic material surfaces," *Archive for Rational Mechanics and Analysis*, vol. 57, no. 4, pp. 291–323, 1975.

[6] M. E. Gurtin and A. Ian Murdoch, "Surface stress in solids," *International Journal of Solids and Structures*, vol. 14, no. 6, pp. 431–440, 1978.

[7] S. Tirapat, T. Senjuntichai, and J. Rungamornrat, "Influence of surface energy effects on elastic fields of a layered elastic medium under surface loading," *Advances in Materials Science and Engineering*, vol. 2017, 2017.

[8] P. Intarit, T. Senjuntichai, and R. K. N. D. Rajapakse, "Dislocations and internal loading in a semi-infinite elastic medium with surface stresses," *Engineering Fracture Mechanics*, vol. 77, no. 18, 2010.

[9] P. Intarit, T. Senjuntichai, J. Rungamornrat, and R. K. N. D. Rajapakse, "Penny-shaped crack in elastic medium with surface energy effects," *Acta Mechanica*, vol. 228, no. 2, 2017.

[10] J. Rungamornrat, S. N. Nguyen, S. Wongthongsiri, K. Panupattanapong, T. Senjuntichai, and B. T. Nguyen, "FE solutions of near-tip field for mode-I cracks with residual surface tension," *ASEAN Engineering Journal*, vol. 9, no. 2, pp. 28-43, 2019.

[11] Y. Yang, Z. L. Hu, A. Gharahi, P. Schiavone, and X. F. Li, "Torsion of an elastic medium containing a nanosized penny-shaped crack with surface effects," *International Journal of Fracture*, vol. 231, no. 2, pp. 189-199, 2021.

[12] Y. Yang, P. Schiavone, and X. F. Li "Torsional deformation of an infinite elastic solid weakened by a penny-shaped crack in the presence of surface elasticity and Dugdale plastic zone," *International Journal of Solids and Structures*, vol. 254, p. 111858, 2022.

[13] P. Intarit, T. Senjuntichai, and J. Rungamornrat, "Elastic layer under axisymmetric indentation and surface energy effects," *Zeitschrift für angewandte Mathematik und Physik*, vol. 69, no. 2, pp. 1–19, 2018.

[14] S. Tirapat, T. Senjuntichai, J. Rungamornrat, and R. K. N. D. Rajapakse, "Indentation of a nanolayer on a substrate by a rigid cylinder in adhesive contact," *Acta Mechanica*, vol. 231, no. 8, 2020.

[15] P. Intarit, T. Senjuntichai, J. Rungamornrat, and S. Limkatanyu, "Influence of frictional contact on indentation of elastic layer under surface energy effects," *Mechanics Research Communications*, vol. 110, p. 103622, 2020.

[16] Y. Sapsathiarn and R. K. N. D. Rajapakse, "Mechanistic models for nanobeams with surface stress effects," *Journal of Engineering Mechanics*, vol. 144, no. 11, 2018.

[17] T. B. Nguyen, J. N. Reddy, J. Rungamornrat, J. Lawongkerd, T. Senjuntichai, and V. H. Luong, "Nonlinear analysis for bending, buckling and post-buckling of nano-beams with nonlocal and surface energy effects," *International Journal of Structural Stability and Dynamics*, vol. 19, no. 11, 2019.

[18] L. H. He, C. W. Lim, and B. S. Wu, "A continuum model for size-dependent deformation of elastic films of nano-scale thickness," *International Journal of Solids and Structures*, vol. 41, no. 3–4, pp. 847–857, 2004.

[19] C. W. Lim and L. H. He, "Size-dependent nonlinear response of thin elastic films with nano-scale thickness," *International Journal of Mechanical Sciences*, vol. 46, no. 11, pp. 1715–1726, 2004.

[20] R. R. Dingreville, J. Qu, and M. Cherkaoui, "Surface free energy and its effect on the elastic behavior of nano-sized particles, wires and films," *Journal of the Mechanics and Physics of Solids*, vol. 53, pp. 1827–1854, 2005.

[21] R. D. Mindlin and H. F. Tiersten, "Effects of couple-stresses in linear elasticity," Archive *for Rational Mechanics and Analysis*, vol. 11, no. 1, pp. 415–448, 1962.

[22] R. A. Toupin, "Theories of elasticity with couple-stress," *Archive for Rational Mechanics and Analysis*, vol. 17, no. 2, pp. 85–112, 1964.

[23] R. D. Mindlin, "Micro-structure in linear elasticity," *Archive for Rational Mechanics and Analysis*, vol. 16, no. 1, pp. 51–78, 1964.

[24] A. Li, X. Ji, S. Zhou, L. Wang, J. Chen and P. Liu "Nonlinear axisymmetric bending analysis of strain gradient thin circular plate," *Applied Mathematical Modelling*, vol. 89, pp. 363-380, 2021.

[25] T. M. Le, D. Vo, J. Rungamornrat, and T. Q. Bui "Strain-gradient theory for shear deformation free-form microshells: Governing equations of motion and general boundary conditions," *International Journal of Solids and Structures*, vol. 248, p. 111579, 2022.
[26] A. C. Eringen, "Nonlocal polar elastic continua," *International Journal of Engineering Science*, vol. 10, no. 1, 1972.
[27] A. C. Eringen and D. G. B. Edelen, "On nonlocal elasticity," *International Journal of Engineering Science*, vol. 10, no. 3, pp. 233–248, 1972.
[28] P. V. Vinh and A. Tounsi "The role of spatial variation of the nonlocal parameter on the free vibration of functionally graded sandwich nanoplates," *Engineering with Computers*, 2021.
[29] H. Bouafia, A. Chikh, A. A. Bousahla, F. Bourada, H. Heireche, A. Tounsi, K. H. Benrahou, A. Tounsi, M. M. Al-Zahrani, and M. Hussain "Natural frequencies of FGM nanoplates embedded in an elastic medium," *Advances in Nano Research*, vol. 11, no. 3, 2021.
[30] A. Garg, M. O. Belarbi, A. Tounsi, L. Li, A. Singh and T. Mukhopadhyay "Predicting elemental stiffness matrix of FG nanoplates using Gaussian process regression based surrogate model in framework of layerwise model," *Engineering Analysis with Boundary Elements*, vol. 143, pp. 779-795, 2022.
[31] P. V. Vinh and A. Tounsi, "Free vibration analysis of functionally graded doubly curved nanoshells using nonlocal first-order shear deformation theory with variable nonlocal parameters," *Thin-Walled Structures*, vol. 174, p. 109084, 2022.
[32] G. Liu, S. Wu, D. Shahsavari, B. Karami and A. Tounsi, "Dynamics of imperfect inhomogeneous nanoplate with exponentially-varying properties resting on viscoelastic foundation," *European Journal of Mechanics - A/Solids*, vol. 95, p. 104649, 2022.
[33] P. V. Vinh, A. Tounsi, and M. O. Belarbi, "On the nonlocal free vibration analysis of functionally graded porous doubly curved shallow nanoshells with variable nonlocal parameters," *Engineering with Computers*, 2022.
[34] P. Lu, L. H. He, H. P. Lee, and C. Lu, "Thin plate theory including surface effects," *International Journal of Solids and Structures*, vol. 43, no. 16, pp. 4631–4647, 2006.
[35] K. F. Wang and B. L. Wang, "Effects of residual surface stress and surface elasticity on the nonlinear free vibration of nanoscale plates," *Journal of Applied Physics*, vol. 112, no. 1, 2012.
[36] C. Liu and R. K. N. D. Rajapakse, "A size-dependent continuum model for nanoscale circular plates," *IEEE Transactions on Nanotechnology*, vol. 12, no. 1, pp. 13–20, 2013.
[37] Y. Sapsathiarn and R. K. N. D. Rajapakse, "Finite-element modeling of circular nanoplates," *Journal of Nanomechanics and Micromechanics*, vol. 3, no. 3, pp. 59–66, 2013.
[38] R. Ansari and R. Gholami, "Size-dependent modeling of the free vibration characteristics of postbuckled third-order shear deformable rectangular nanoplates based on the surface stress elasticity theory," *Composites Part B: Engineering*, vol. 95, pp. 301–316, 2016.
[39] Y. Yang, J. Zou, K. Y. Lee, and X.F. Li, "Bending of circular nanoplates with consideration of surface effects," *Meccanica*, vol. 53, pp. 985-999, 2018.
[40] Y. Yang and X. F. Li, "Bending and free vibration of a circular magnetoelectroelastic plate with surface effects," *International Journal of Mechanical Sciences*, vol. 157-158, pp. 858-871, 2019.
[41] E. Winkler, "Die Lehre von der Elasticitaet und Festigkeit: mit besonderer Rücksicht auf ihre Anwendung in der Technik," für polytechnische Schulen, Bauakademien, 1867.
[42] P. L. Pasternak, "On a new method of analysis of an elastic foundation," Gos. Izd. Lip. po Straiti Arkh, Moscow, 1954.
[43] A. M. Zenkour and M. Sobhy, "Nonlocal elasticity theory for thermal buckling of nanoplates lying on Winkler–Pasternak elastic substrate medium," *Physica E: Low-dimensional Systems and Nanostructures*, vol. 53, pp. 251–259, 2013.
[44] M. Sobhy and A. M. Zenkour, "Nonlocal thermal and mechanical buckling of nonlinear orthotropic viscoelastic nanoplates embedded in a visco-pasternak medium," *International Journal of Applied Mechanics*, vol. 10, no. 8, 2018.
[45] Q. Li, D. Wu, W. Gao, and F. Tin-Loi, "Size-dependent instability of organic solar cell resting on Winkler–Pasternak elastic foundation based on the modified strain gradient theory," *International Journal of Mechanical Sciences*, vol. 177, p. 105306, 2020.
[46] F. Kamali and F. Shahabian, "Analytical solutions for surface stress effects on buckling and post-buckling behavior of thin symmetric porous nano-plates resting on elastic foundation," *Archive of Applied Mechanics*, vol. 91, no. 6, pp. 2853–2880, 2021.
[47] J. N. Reddy, *Energy Principles and Variational Methods*. 2020.
[48] A. P. S. Selvadurai, *Elastic Analysis of Soil-Foundation Interaction*. 1979.
[49] A. D. Kerr, "Elastic and viscoelastic foundation models," *Journal of Applied Mechanics*, vol. 31, no. 3, pp. 491–498, 1964.
[50] D. E. Barton, M. Abramovitz, and I. A. Stegun, "Handbook of mathematical functions with formulas, graphs and mathematical tables," *Journal of the Royal Statistical Society. Series A (General)*, vol. 128, no. 4, 1965.
[51] Y.-Y. Yu, "Axisymmetrical bending of circular plates under simultaneous action of lateral load, force in the middle plane, and elastic foundation," *Journal of Applied Mechanics*, vol. 24, no. 1, 1957.
[52] V. B. Shenoy, "Atomistic calculations of elastic properties of metallic fcc crystal surfaces," *Physical Review B - Condensed Matter and Materials Physics*, vol. 71, no. 9, 2005.

DOI:10.4186/ej.2022.26.10.99

Supakorn Tirapat was born in Ubon Ratchathani, Thailand in 1990. He received the Bachelor Degree in Civil Engineering from Khon Kaen University, Khon Kaen, Thailand in 2012, and the Doctor of Philosophy in Civil Engineering from Chulalongkorn University, Bangkok, Thailand in 2018.

Since 2018, he has been an instructor with Department of Civil Engineering, Faculty of Engineering, Khon Kaen University, Khon Kaen, Thailand. His research interests include solid and structural mechanics, computational modelling, applied mechanics, contact mechanics, civil engineering.

Teerapong Senjuntichai obtained his B. Eng. (Civil Engineering) from Chulalongkorn University in 1988; M. Eng. (Structural Engineering) from Asian Institute of Technology in 1990; and Ph.D. (Civil Engineering) from The University of Manitoba in 1994. He has then joined the Department of Civil Engineering, Chulalongkorn University, where he is currently a full-time professor. He was a post-doctoral associate at The University of Minnesota from 1997-1999. His fields of specialization are solid and structural mechanics. He has served as a Section Editor for ASEAN Engineering Journal, an editorial board member for Songklanakarin Journal of Science and Technology and Journal of the Civil Engineering Forum, and a Head of Center of Excellence in Applied Mechanics and Structures, Chulalongkorn University.